

AN EFFICIENT SEISMIC NONLINEAR SSI APPROACH BASED ON BEST PRACTICES IN US AND JAPAN. PART 1: MODELING

Dan M. Ghiocel¹, Yasuo Nitta² and Ryosuke Ikeda³ and Tatsuhiro Shono⁴

¹ President, Ghiocel Predictive Technologies, Inc., New York, USA (dan.ghiocel@ghiocel-tech.com)

² Senior Engineer, SHIMIZU Corporation, Tokyo, Japan (nitta_y@shimz.co.jp)

³ General Manager, SHIMIZU Corporation, Tokyo, Japan (ikedar@shimz.co.jp)

⁴ Structural Engineer, Terrabyte Corporation, Tokyo, Japan (tatsuhiro.shono@terrabyte.co.jp)

ABSTRACT

The paper introduces an efficient nonlinear seismic SSI approach for evaluating the reinforced concrete (RC) shearwall structures behaviour under severe earthquakes in accordance with the engineering practices and regulatory requirements in US and Japan. The nonlinear SSI approach is based on a hybrid approach that uses an iterative scheme which couples the equivalent-linear complex frequency SSI analysis with the nonlinear time-domain structure analysis. The iterative approach is fast converging in only few SSI restart iterations. The SSI approach implementation follows the Japanese seismic nonlinear analysis engineering practice extended to detailed 3DFEM SSI models. The implementation is compliant with the RC wall structure modeling standard requirements in US and Japan. Independent verifications and validation studies confirmed that the iterative SSI approach is reasonably accurate and extremely numerically efficient. There are two companion papers, Part 1 and Part 2, related to the iterative SSI approach: The Part 1 paper focuses on the key modeling aspects for capturing nonlinear hysteretic behavior of RC structure walls, while the Part 2 paper focuses on its application using the ACS SASSI Option NON software.

INTRODUCTION

This Part 1 paper introduces the iterative hybrid SSI approach and discusses key assumptions of the nonlinear modeling of the RC wall structure behavior under damaging earthquakes. The approach implementation follows the Japanese seismic nonlinear analysis engineering practice extended to detailed 3DFEM SSI models. The nonlinear RC structure modeling is compliant with the requirements of the seismic analysis and design standards in US and Japan. Specifically, the ACI 318-19 and ASCE 4-16 standards in US and the JEAC 4601-2015 and the AIJ RC 2018 standard requirements are considered. The nonlinear SSI approach was implemented a while ago in the ACS SASSI Option NON software (GP Technologies, 2022) and it has been already verified over a period of seven years against actual design projects in Japan, different specialized RC structure software packages and different experimental RC wall tests (Ghiocel, 2015, Ghiocel et al., 2022, Nitta et al., 2022). More recent independent verification and validation studies were performed by Nuclear Regulation Authority of Japan and Japan Atomic Energy Agency comparing results against the NUPEC experimental wall test data and sophisticated nonlinear FE time-domain analysis results (from IAEA KARISMA project). These independent verification studies indicated that the iterative hybrid SSI approach provides a reasonable accuracy with a high numerical efficiency (Ichihara et al., 2021, 2022).

BASIC CONCEPT OF ITERATIVE HYBRID SSI APPROACH

Computational Steps

Figure 1 describes the concept of the iterative SSI approach. The nonlinear SSI analysis based on the iterative hybrid approach includes at each iteration two separate coupled analysis steps:

Step 1: Perform an *equivalent-linear SSI analysis* in complex frequency via SASSI approach to compute the structural displacements for each nonlinear RC wall, and then,

Step 2: Perform a *nonlinear time-integration analysis* for each RC wall loaded with the SSI displacements from Step 1, to compute the in-plane shear and bending nonlinear wall responses using *standard-based back-bone curve (BBC) equations* and *appropriate hysteretic models from the software library*.

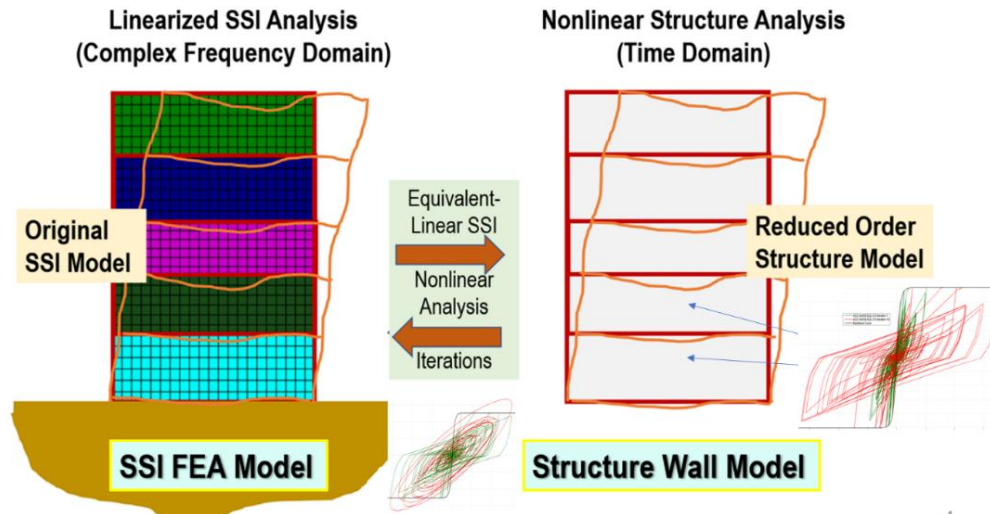


Figure 1 Iterative Hybrid SSI Approach Concept Implemented in ACS SASSI Option NON

The *equivalent-linear stiffness and damping for each RC wall* are computed based on time domain nonlinear responses using either a constant or variable displacement reduction factor (DRF) applied to each SSI iteration. It should be noted that *Step 1* uses the *original, refined FE SSI model*, while *Step 2* uses a *reduced-order structural model* using macro-mechanics hysteretic models for simulating the RC wall behaviour. These macro models are called wall panels and include all groups of the shell elements defining the wall geometry at each floor level (see the wall panels in different colours in Figure 1 right plot). The wall panels include the wall cross-section web and its eventual flanges (as shown later in Figure 6). Therefore, the Step 2 “true” nonlinear time-domain integration analysis is extremely fast. The reduced-order model idealizes the RC shearwall structure nonlinear behaviour by using a macro-mechanics hysteretic modelling for each wall panel. These nonlinear wall panels are defined at each floor level (differently colored in Figure 1) are assumed to be subjected to uniform shear and bending deformation patterns. For 3DFEM models, the nonlinear wall panels are usually modelled by thick shell elements, while for the SR/Stick models, the nonlinear wall panels are modelled by pairs of translational and rotational springs.

The main steps of the iterative SSI approach applied to a 3DFEM, as implemented in the ACS SASSI Option NON software, are as follows:

1. Prepare structure 3DFEM model
2. For selected nonlinear RC walls create 3DFEM submodels
3. Perform linear SSI analysis for gravity and seismic loads to compute structural stresses
4. Perform RC wall cross-section geometry identification for all floor levels at defined sections
5. Perform automatic section-cuts for each wall for gravity and three direction seismic loads
6. Compute shear and bending back-bone curves (BBC) for each wall and floor level *per* applicable best-practice recommendations in US or Japan
7. Select appropriate shear and bending hysteretic models from the software library per applicable best-practice recommendations in US or Japan
8. Perform SSI and nonlinear analysis iterations using shear and bending hysteretic wall models
9. Combine the computed interacting shear and flexure responses after each iteration
10. Optionally, include the floor concrete cracking due to the bending effects under vertical motion
11. Post-process the final SSI results of 3DFEM for the converged nonlinear response

The nonlinear SSI analysis based on the iterative hybrid approach is applicable to i) Design Basis Earthquake (DBE) projects for evaluating the RC cracking pattern in structures, and ii) Beyond Design Basis Earthquake (BDBE) projects for evaluating the RC wall post-cracking and yielding behaviour

until ultimate limit state is reached. Useful examples including DBE and BDBE applications are presented elsewhere (Ghiocel, 2022, Ghiocel et al., 2022, Nitta et al., 2022).

Displacement Reduction Factors

Displacement Reduction Factors (DRFs) are used to ensure the convergence of iterative equivalent-linearization schemes for modeling nonlinear material hysteretic behavior. Since the RC wall stiffness is degraded during severe earthquakes, its effective or equivalent-linear stiffness is iteratively reduced based on the DRF as shown in Figure 2. The DRF is defined as the ratio between the effective displacement, D_{eff} , and maximum displacement, D_{max} . This DRF ratio can be defined with a constant or variable value at each iteration based on the modification of the wall panel (at each floor) nonlinear response frequency content. Therefore, the DRF value at each iteration can be either: 1) Constant DRF values for all iterations, or 2) Variable DRF values computed at each iteration. The constant DRF value is a user-defined input (with a best estimate about 0.80 value). For the variable DRF value, at each iteration the equivalent wall stiffness is computed using the ratios between the frequencies of the dominant spectral peaks of the power spectral density (PSD) functions computed for the nonlinear panel shear forces or moments in the current iteration versus the previous iteration. The DRF values which correspond to the panel stiffness degradation ratios that are computed by the square of the PSD dominant frequency ratios. Then, the hysteretic damping is computed based on the energy loss per cycle by approximating hysteretic loop area with an equivalent viscous damping ellipse as shown in Figure 2.

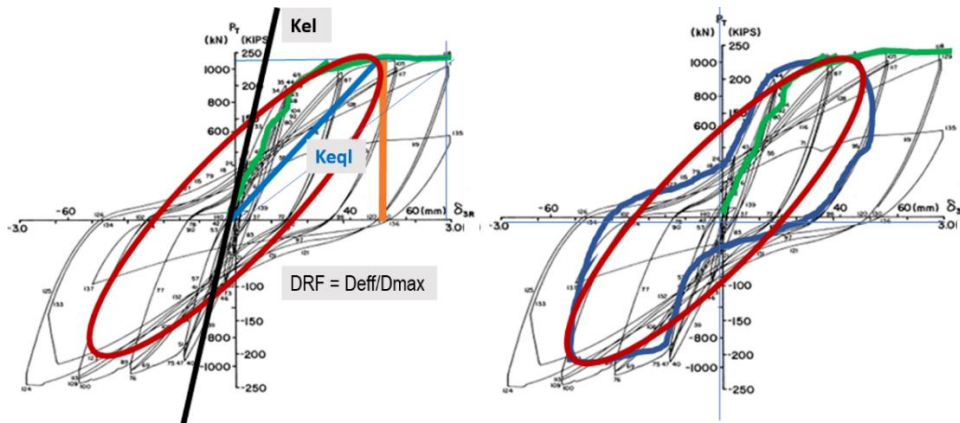


Figure 2 Computation of Equivalent RC Wall Stiffness and Damping Based on DRF at Each Iteration

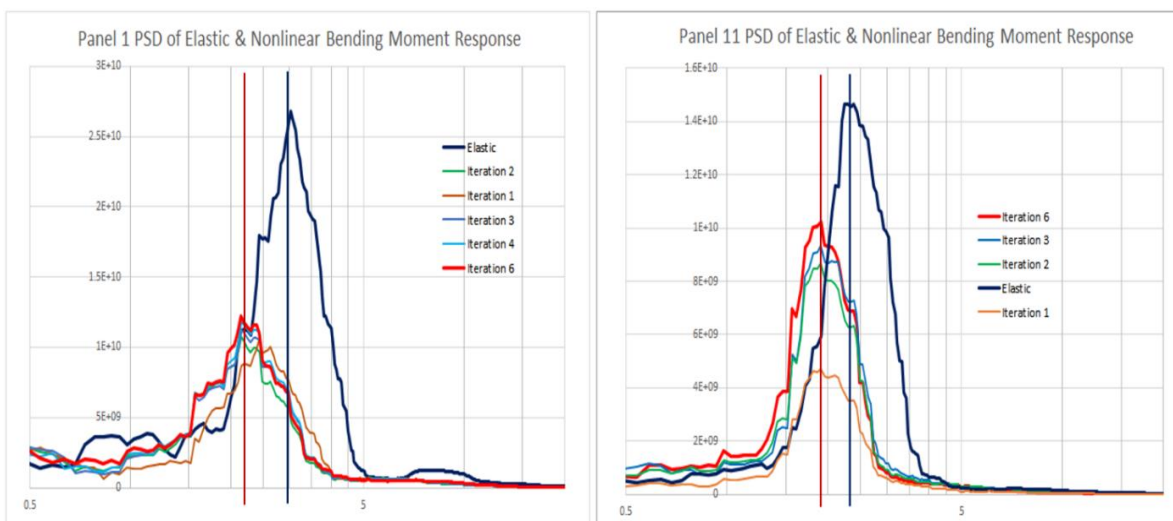


Figure 3 Two Wall Panel Nonlinear Moment PSD Functions at Selected Iterations Until Convergence

It should be noted that the computation of the equivalent viscous damping based on the closed hysteretic loops is not applicable in conjunction with the Japanese hysteretic maximum point-oriented models

recommended by JEAC 4601 App. 3.7 which have a zero-area for hysteretic closed loops, as discussed hereafter and elsewhere (Ghiocel et al., 2022, Nitta et al., 2022).

Figure 3 shows typical iterative variations of the PSD frequency content of the nonlinear wall panel bending moment. The vertical lines show the overall shifts of the dominant panel frequency due the wall panel nonlinear behavior, from the initial linear elastic SSI analysis to the final converged iterated SSI analysis. Figure 3 also indicates that a reasonably converged nonlinear solution can be obtained in only 2-3 iteration steps. If the FVROM-INT approach is used, each iteration takes a fraction of the initial linear SSI analysis (Ghiocel, 2022).

It should be noted that for typical RC structures, the use of a constant DRF value of 0.80 or a variable DRF value for each panel and iteration affects only minorly the nonlinear SSI converged solution as shown in Figure 4 for a nonlinear shear force in a RC wall and an ISRS at a structure high elevation. The variable DRF is activated when the user input for DRF is equal to zero.

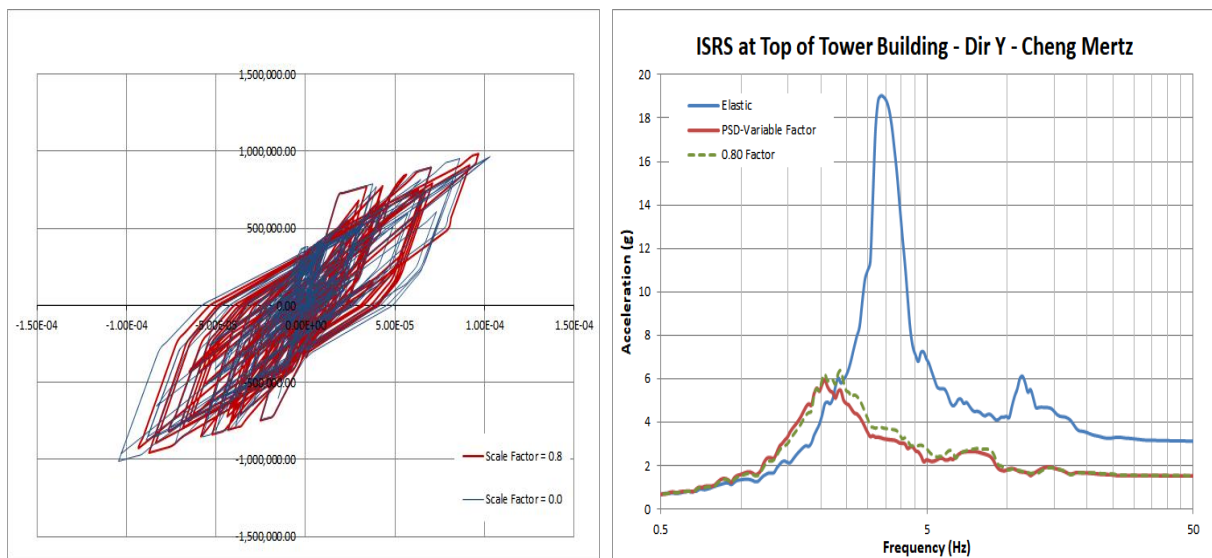


Figure 4 Effects of Constant DRF (= 0.80) vs. PSD-Based Variable DRF (=0) on Nonlinear Responses
Shear and Bending Back Bone Curves (BBC) for RC Walls

To compute the nonlinear wall shear and bending deformation at for each iteration, the computed displacements of wall panel corner nodes are used. The wall panel in-plane shear and bending deformations are derived from the vertical edge relative rotation and, respectively, the relative horizontal edge rotation of the panel at each time step. Their time variations along the panel length and height are derived assuming linear variations. Based on the computed panel relative rotation, the panel *bending curvature* and the panel bending horizontal displacement are obtained by derivation and, respectively, integration along the panel height. The panel shear displacement is determined by subtracting the panel bending displacement from the panel total horizontal displacement, and then, the panel *shear strain* is computed by normalizing the panel shear displacement to the panel height (between the top and bottom floor levels).

For performing the nonlinear structure SSI analysis for the general case, the user is required to determine the wall panel constitutive material curves or BBC for the shear and bending deformation. For the RC walls, the in-plane shear force-shear strain relationship for shear BBCs, and the in-plane bending moment-curvature relationship for bending BBCs should be determined for each wall panel. Two options are available for creating the shear and bending BBCs: 1) User-defined BBCs, and 2) Automatically computed BBCs based on either US or Japan standards or a 3D fiber interactive model.

For the low-rise RC shearwall structures, which are governed by the shear effects, the shear BBCs can be automatically computed by empirical equations applicable to the plane wall shear capacities, which are acceptable in US practice, such as the Gulec-Whittaker, Wood, ACI 318, and Barda equations (Gulec and Whittaker, 2009).

For general case of RC shearwall structures for which both shear and bending effects might be significant, there is the option to automatically compute shear and bending BBCs based on either the US standards (ACI 318-19 and ASCE 4-16) or the Japan standards (JEAC 4601-2015 and AIJ RC 2018). The automatically generated panel BBCs are provided as trilinear curves defined by three relevant points, the point 1 for concrete cracking limit, the point 2 for yielding limit state, and the point 3 for ultimate limit state.

The effects of the vertical axial forces due to the gravity (static) loads are also included for computing the BBCs, as indicated by the US or Japan standard. The yielding moment, M_y , and the ultimate moment, M_u , are computed using standard design calculations in compliance to ACI 318 and JEAC 4601 standards, as shown in Figure 5.

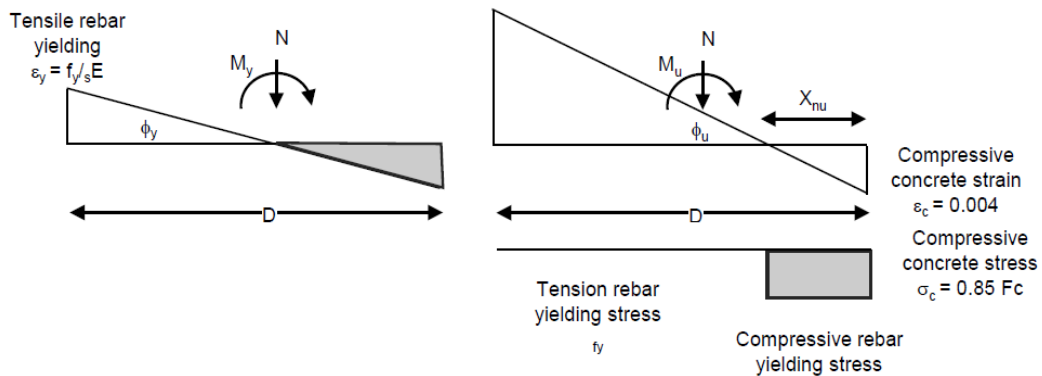


Figure 5 Basic Assumptions for Cross-Section Calculations for M_y and M_u Moments

It should be noted that for standard RC wall cross-section shapes, as I, C, T shapes, the wall section geometric properties, required to compute the sectional BBC at each floor level, are automatically identified based on the FE model mesh geometry, as shown in Figure 6 left. The RC wall section web and flanges are computed in accordance with the standard requirements for effective flange sizes, including openings and different pier thicknesses as shown in Figure 6 right (GP Technologies, 2022).

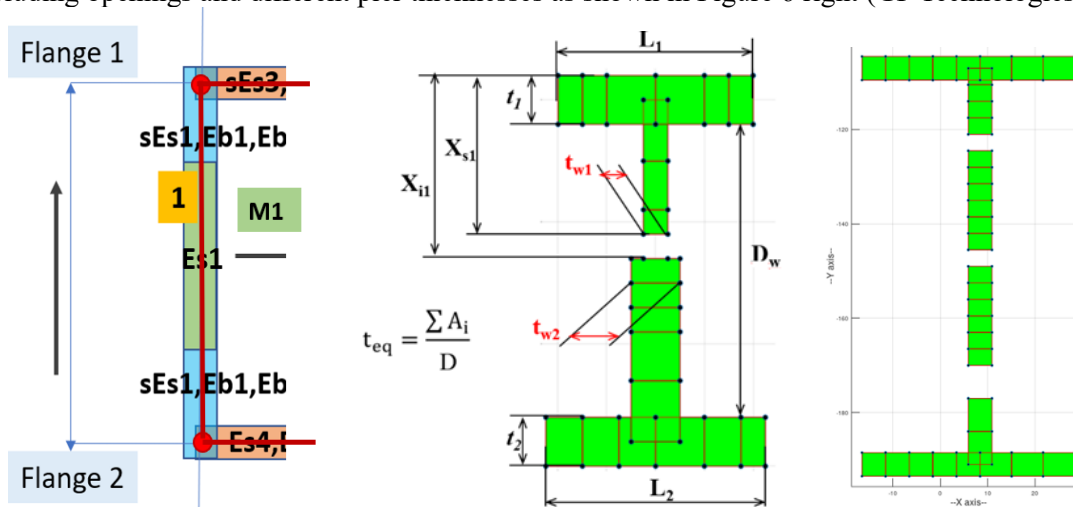


Figure 6 Automatic Identification of RC Wall Cross-Section Shape Based on the Submodel FE Mesh

The RC wall reinforcement is input based on the user-defined percentage ratios in the vertical direction for flanges, and the vertical and horizontal directions for web (Figure 7). Usually, one to few layers of distributed steel bars is considered. For the wall intersections, the reinforcement is lumped in the center.

Alternatively, user can consider more detailed reinforcement description including locations of the individual vertical corner or edge bars and the horizontal stirrup bars. The Eurocode EC2 and Mander concrete models are available in conjunction with the use of a 3D wall fiber model (Spacone et al, 1992) which is applicable to any wall cross-section shapes.

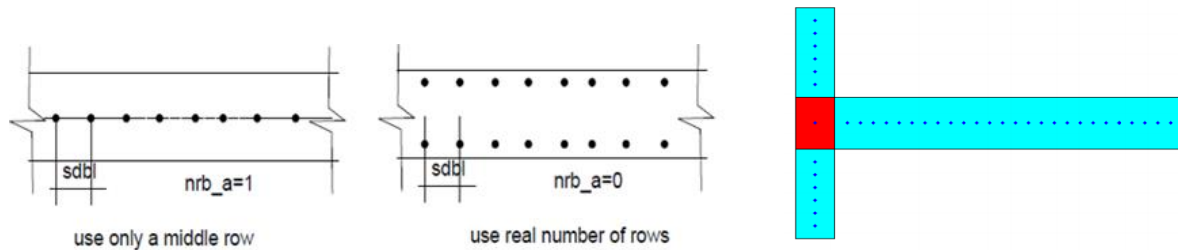


Figure 7 Typical Reinforcement Distributed Pattern for RC Walls (No Individual Corner Bars)

To compute the wall BBCs at each floor level, sectional forces, N and V (N = gravity axial forces and V = seismic shear forces), and moments, M (M = seismic bending moment), are determined using an automatic section-cut algorithm.

Typical shear and bending BBCs computed for an exterior RC wall with a C-shaped cross-section are shown in Figure 8. As shown in Figure 8, the shear BBC based on JEAC 4601 App.3.7 equations are well above the BBC based on ACI 318-19 equations, with the largest difference noted for the ultimate state point. The effects of the wall flanges to increase the overall wall shear capacities is considerably larger for the JEAC 4601 App.3.7 equations. It should be noted that the BBC equations per JEAC 4601 include the interactive effects due the axial force N , shear force V , and bending moment M . In contrast to JEAC 4601, the ACI 318 in-plane wall shear capacity (ultimate state point of trilinear shear BBC) is computed without considering the shear force-bending interaction or the shear force-axial force interaction. At the same time, it should be remarked that the ultimate shear strain for the low-rise walls in JEAC 4601 App.3.7 is limited to 0.004 that corresponds to only damage limit state C in ASCE 43-19 Chapter 5. The bending BBCs vary uniformly with height since the considered TB (tower building) structure with five floors has a simple rectangular layout with the same wall clearance for all floor levels.

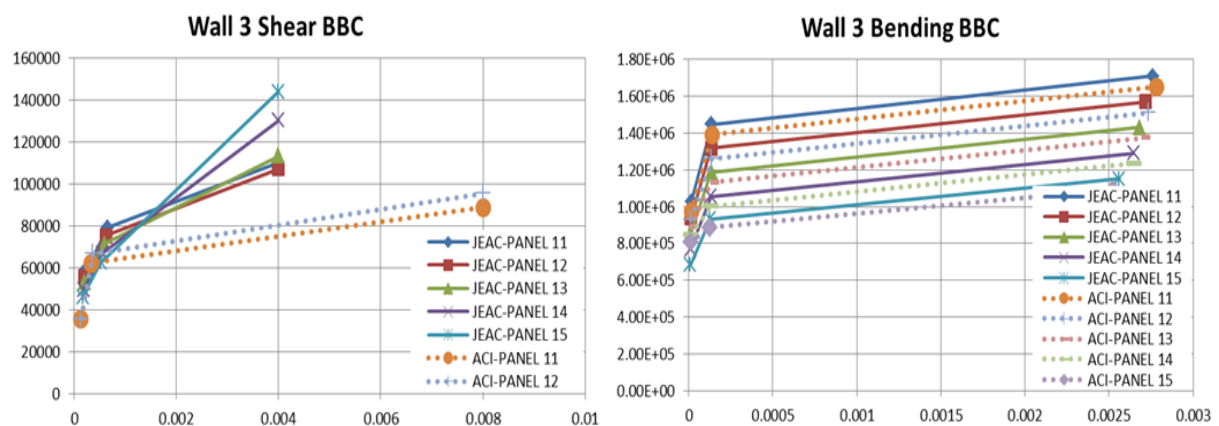


Figure 8 Comparative TB Building Shear and Bending BBCs for Exterior Wall for All Floor Levels

It should be noted that JEAC 4601 BBC equations were established for a variety of RC wall cross-section shapes, not only for plane walls. The tested RC wall shapes in Japan include in addition to plane walls, flanged walls and closed section walls (Figures 9) as reported by Taitokui (Taitokui, 1987).

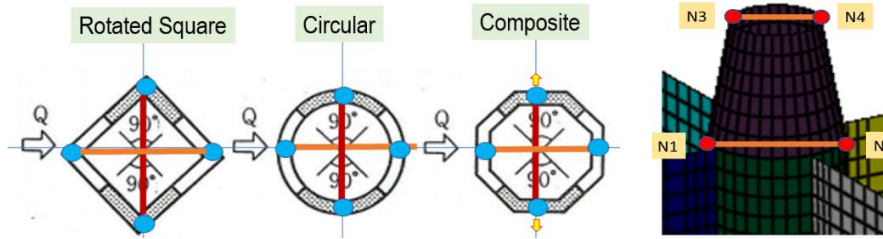


Figure 9 Elementary Section Shapes for Some of RC Walls Tested in Japan (Taitokui, 1987)

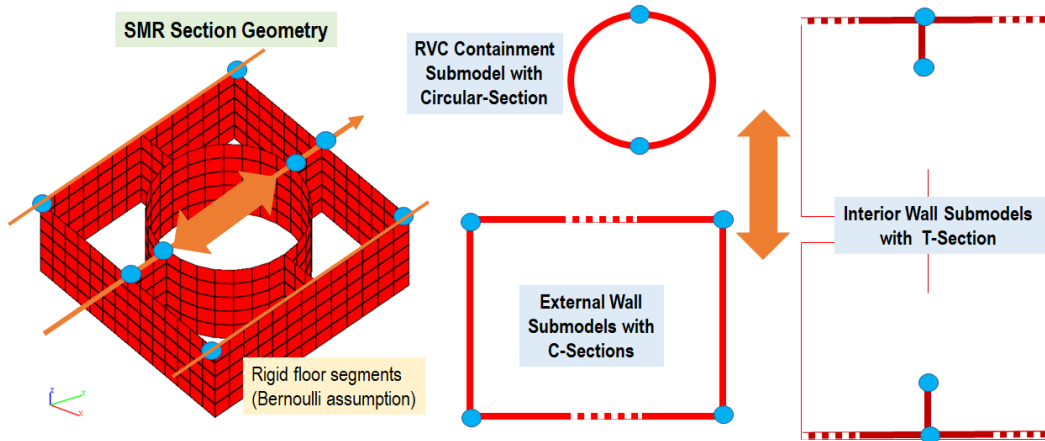


Figure 10 Composite Shape RC Wall Split in Elementary Shape RC Walls

To handle the BBC computation for non-standard plane RC wall, a refined 2D-section fiber model was implemented based on the original 3D fiber model by Spacone (Spacone et al., 1992). Therefore, the BBC calculations are not limited to the standard plane walls with or without flanges, but can be also done for closed section or composite or even arbitrary section walls, as illustrated in Figures 9 and 10.

It should be noted that for complex wall cross-section shapes including non-planar walls, the panels could be split in several elementary shaped panel segments, each satisfying the beam theory by assuming rigid bottom-top floor panel edges. For these complex configuration walls, the 2D-section fiber model is applied for computing bending BBCs, and a numerical integration algorithm is applied for computing the shear BBCs (GP Technologies, 2022). The shear BBC are computed based on the computed section shear area for each horizontal direction, as shown by the shadowed areas in Figure 9.

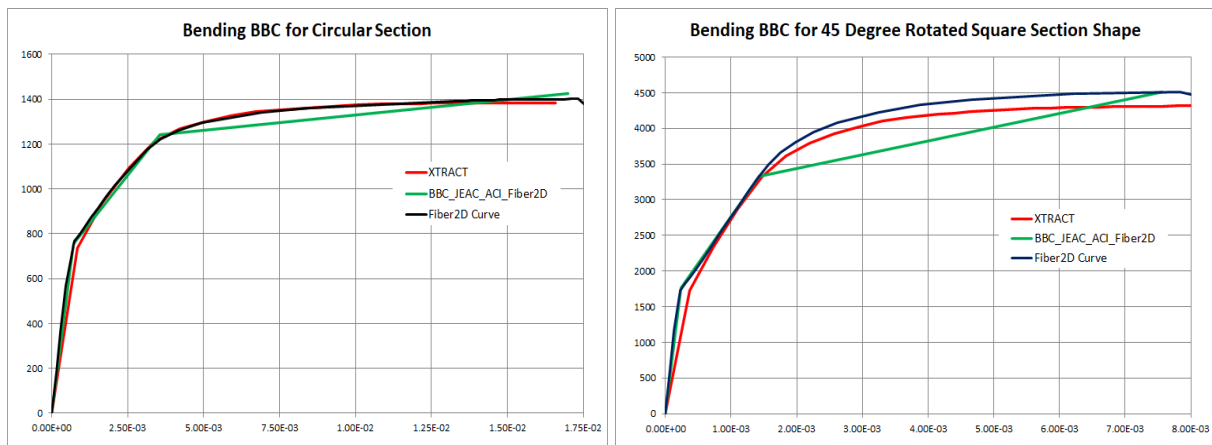


Figure 11 Circular and Rotated Square Section Bending BBCs Computed with 2DFiber and XTRACT

Figure 11 shows a comparison between trilinear bending BBC computed with the 2D-section fiber model for a circular wall and a rotated square wall (Figure 9) and smooth BBC computed with the 2D-

section fiber model and the specialized XTRACT software (Chadwell and Imbsen, 2004) for the RC structures shown in Figure 10. The EC2 concrete model with a non-zero tension strength was considered for the 2D-section fiber model. No concrete tension strength was considered for XTRACT input.

Shear and Bending Hysteretic Effects Interaction

The RC wall nonlinear behaviour occurs under horizontal seismic components that produce large shear and bending in-plane deformation. Under vertical seismic component, no or minor wall stiffness degradation is expected under the gravity and seismic loads.

The nonlinear SSI results are based on combining in 3D space the nonlinear SSI analysis displacements under the horizontal seismic components with the linear SSI analysis under vertical gravity and seismic loads. The shell element material isotropy assumption is maintained during the iterations which implies that the panel shear or bending hysteretic stiffness modifications impact proportionally to other wall panel stiffnesses assumed to be a Kirchhoff shell. Alternatively, a transverse orthotropic material can be defined for capturing the reduction in the transverse shear stiffness within the Mindlin shell formulation. The orthotropic material is also useful for modelling the steel-concrete (SC) wall behaviour.

There are two hysteretic type elementary behaviours for a RC wall panel at each iteration: 1) Shear-governing hysteretic behaviour and 2) Bending-governing hysteretic behaviour. However, for the general RC wall case for which the shear and bending deformation effects are both significant, the interaction between the hysteretic shear and bending effects can be incorporated for each panel at each iteration.

The experimental evidence from a series of planar RC wall tests at the LANL and NCKU laboratories indicated that the use of an ellipsoidal shaped interaction curve for the shear force-bending moment effects provides wall capacities which are deviating from the measured capacities by only 3% for the yielding point and 9% for the failure point (Cheng and Mertz, 1989). The ellipsoidal interaction curves are often used in practice. It should be noted that the ellipsoidal interaction curve corresponds to the separation of variable principle that is largely used for the mathematical modelling of complex physical phenomena with separated variability sources. The ellipsoidal curve shape indicates the relative independence between the nonlinear shear and nonlinear bending deformation effects.

Two options are considered for the shear-bending interaction *for each panel at each iteration* based on *the ellipsoidal interaction curve assumption*: 1) Equivalent circle radius (ECR) and 2) Ellipse inclined radius (EIR). If notation E_s is the shear degraded material elastic modulus and E_b is the bending-axial degraded material elastic modulus, then, the ECR option computes the effective E_{sb} modulus (for combined shear and bending effects) at iteration i using the equivalent-linear E moduli computed by the shear and the bending hysteretic models at iteration i and the effective E modulus computed at the previous iteration $i-1$, while EIR option computes the effective E_{sb} modulus at iteration i , using the interaction ellipse radius for equal contributions of the E_s and the E_b of the same iteration i .

It should be noted that the use of the ECR or EIR option affects only negligibly the nonlinear SSI solution accuracy (GP Technologies., 2022).

Figure 12 shows the V-M shear-bending interaction and the N-M axial-bending interactions for the computed response time history results against the limit state V-M and N-M interaction curves (consistent with BBC calcs). The axial forces correspond to the gravity load effects. The two interaction curve lines are for yielding limit state (blue line) and ultimate limit state (red line).

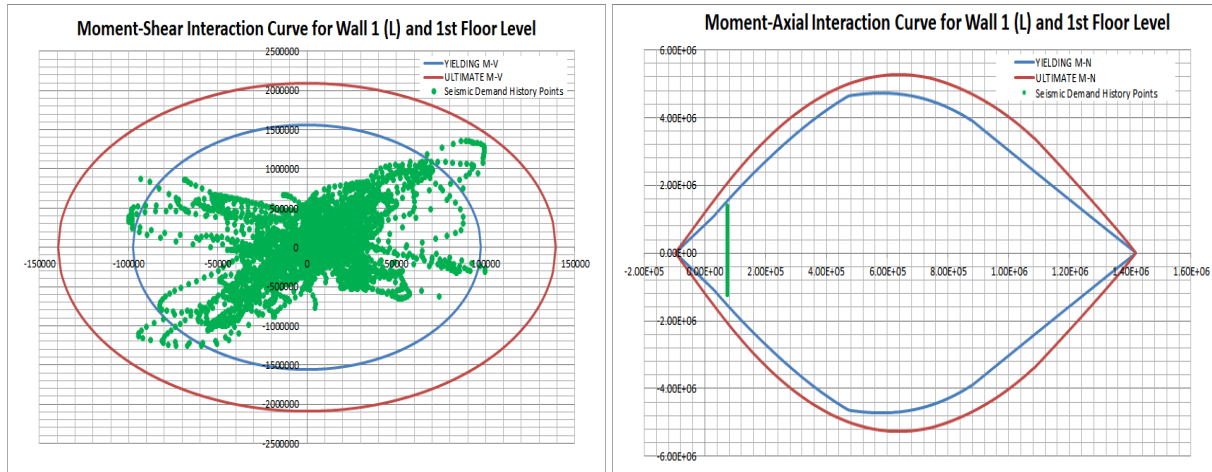


Figure 12 V-M Shear-Bending Interaction (left) and N-M Axial Force-Moment Interaction (right) Diagrams for Iterated Converged Results

It should be noted that the interaction between shear and bending nonlinear effects is conditioned by the fact that at each iteration the shear force is transmitted mostly to the wall web, while the bending moment are transmitted mostly through to the wall flanges. Four nonlinear wall modeling cases are considered. The first three cases apply to simultaneous seismic inputs for X, Y and Z directions, while the last fourth case apply to separate seismic inputs for the X, Y and Z directions.

Case 1: Nonlinear shear and bending effects affect only the wall panel web

Case 2: Nonlinear shear effects affect only the wall webs, while bending effects affect only the wall flanges. The intersected wall panel end flanges are subjected to interaction between biaxial bending and shear along the plane of the wall web.

Case 3: Nonlinear shear effects affect only the wall panel webs, while bending effects affect only the wall flanges. The intersected wall end flanges are subjected to interaction between directional uniaxial bending and shear along the plane of the wall web.

Case 4. Nonlinear shear effects affect only the wall panel webs, while bending effects affect only the wall flanges. For each input direction, the wall webs and flanges are separately subjected to shear effects and bending effects, respectively.

Cases 1-3 are specifically applicable to the 3DFEM models since these cases avoid using the linear superposition of nonlinear responses computed separately computed for X and Y directions, but consider the X, Y and Z inputs as simultaneous seismic inputs. Case 1 uses a simplistic nonlinear model with a complete decoupling between shear and bending effects, while Case 2 and 3 incorporates for the wall flange areas, the biaxial bending-shear interaction effects, or alternatively the directional bending-shear interaction effects. Case 4 is specifically applicable to the Stick/SR models per current JEAC 4601-2015 guidance and past practice in Japan. For Case 4, the analyst should use separate nonlinear SSI models for each input direction. The nonlinear SSI analysis is performed separately and only at the end their results are superimposed. This is a simplified approach since uses the superposition for the two directional model nonlinear responses for X and Y inputs.

For illustration, a Case 3 material modeling for a simple wall geometry configuration is shown Figure 13. In addition to the initial elastic wall panel web materials, separate flange materials are automatically included. The nonlinear flange materials are generated based on specific model geometry and material information and computed effective flange widths based on applicable standard.

During iterations, the nonlinear shear stiffness degradation (effective E is E_s) is assigned to the middle web parts (green), while the nonlinear bending stiffness degradation (effective E is E_b) is assigned to the end flanges (orange-yellow for Y direction and blue for X direction) per JEAC 4601-2015 nonlinear

wall modeling practice.

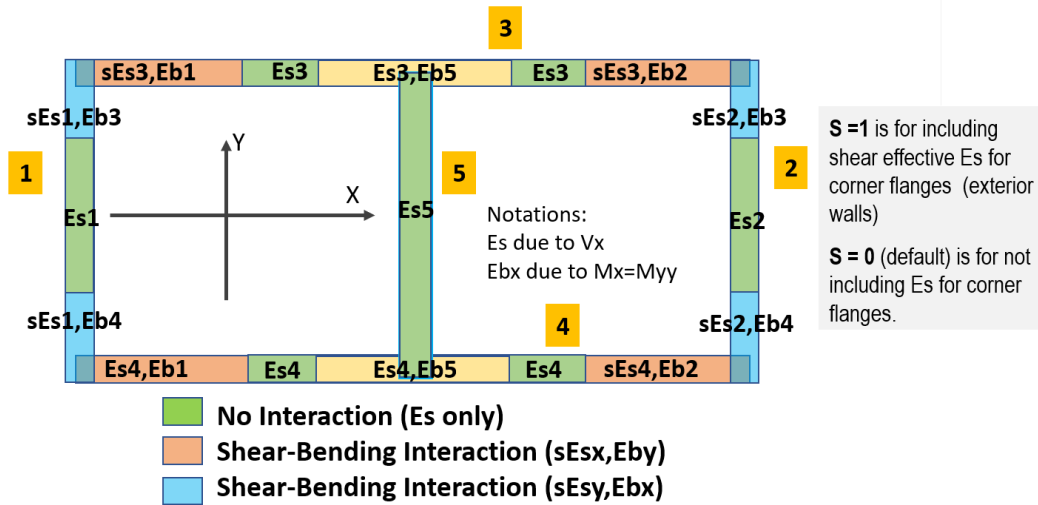


Figure 13 Case 3 With Shear-Bending Interaction; Effective Stiffnesses for Webs and Flanges (Es and Eb) with Assumed Directional Bending (Ebx for X-input and Eby for Y-input are decoupled)

It should be noted that the s coefficient in front of Es in Figure 13 is an optional flag to consider the shear effects for flanges or not. If s=0, then, the shear effects are not included for flange areas, and if s=1, the shear effects are included for flange areas.

The effective flange widths for standard plane walls with C, I, T cross-section shapes are computed based on ACI 318-19 in US, or AIJ RC-2018 in Japan. Figure 14 shows the computed effective wall flanges (with different colors than web colors) for a typical Auxiliary Building (AB) shearwall structure based on the Japanese AIJ RC standard equations. Different clearances were considered for each floor depending on building wall internal layout. Although the ACI 318-19 provides different sizes for the computed effective flange widths that JEAC 4601-2015, the impact on the overall nonlinear structure behaviour is quite limited as shown elsewhere (Ghiocel, 2022).

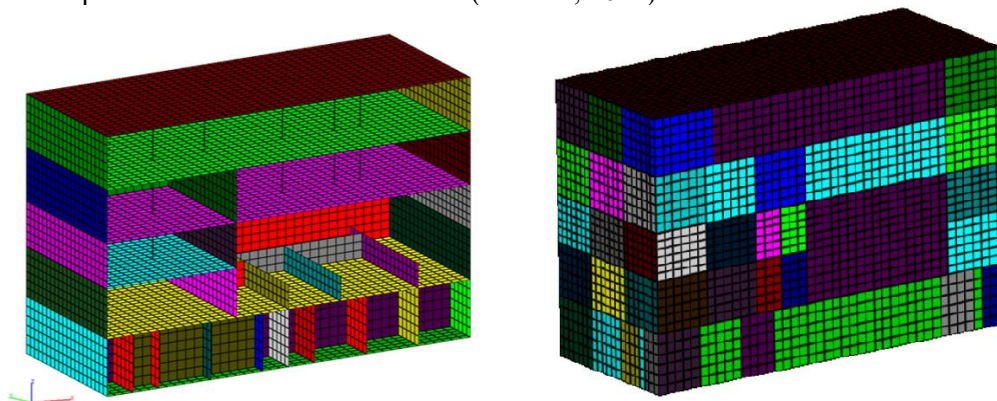


Figure 14 Computed Effective Flanges (right) for AB Shearwall Structure (left) Based on JEAC 4601 & AIJ RC Standard Equations

An example for the Case 3 implementation by automatically introducing new flange materials is shown below in Figure 15. The initial wall web materials are M1-M5 (green), while the added flange materials are M6-M15 (orange, blue and yellow). The M14-M15 (yellow) correspond to the flanges of the interior wall. The exterior wall flanges include only the end flanges and does not include the middle flange that correspond to the interior wall. The nonlinear RC wall flange widths are computed based on the applicable standard requirements, either AC in US, or AIJ RC-2018 in Japan.

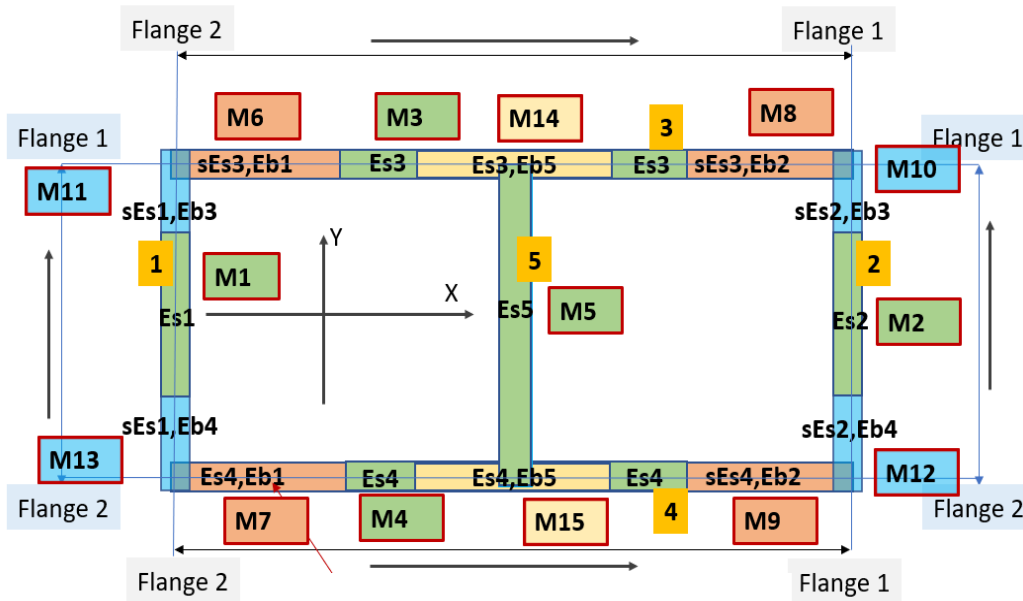


Figure 15 Case 3 Example for Definition of Nonlinear Materials in Webs and Flanges (Es and Eb)

It should be noted that, optionally, the concrete floor cracking effects due to out-of-plane bending can be also included. The floor cracking is checked by computing the element maximum normal stresses at the top and bottom floor slab faces and compare them with the concrete cracking, locally, element by element. The floor cracking effects might be significant for vertical ISRS, and mostly negligible for horizontal ISRS (Ghiocel, 2022).

Simplified Case for Low-rise RC Shearwall Structures

It should be noted that for the low-rise RC shearwalls, the nonlinear structural dynamic behaviour is usually governed by the shear deformation, while bending effects play an insignificant role. Based on various experimental tests done at Cornell University, Gergely points out in NUREG/CR 4123 (Gergely, 1984) that for the low-rise shearwalls such as those that occur in the modern nuclear power plants, the flexural distortions and associated vertical yielding play a negligible role. This was also recognized by many other research studies, including the EPRI report on “Methodology for Developing Seismic Fragilities” (Reed and Kennedy, 1994). Therefore, for the low-rise shearwall structures, the nonlinear structure behaviour could be assumed to be governed the wall panel shear deformation, and the solely use of the shear governing hysteretic models might be sufficient. However, the existence of large openings in the walls that split walls in separate piers may affect the shear-governing assumption. A recent evaluation of the application of the iterative SSI approach based on the shear-governing assumption was performed by Ichihara for the RB complex of the Kashiwazaki– Kariwa ABWR NPP (Ichihara, 2022).

Shear and Bending Hysteretic Model Library

The ACS SASSI Option NON software library includes eight types of hysteretic models that can be used for nonlinear RC wall modeling, as follows:

- 1) Cheng-Mertz Shear (CMS) model (model 1)
- 2) Cheng-Mertz Bending (CMB) model (model 2)
- 3) Takeda (TAK) model (model 3)
- 4) General Massing Rule (GMR) model (model 4)
- 5) JEAC 4601 Maximum Point-Oriented (PO) shear model (model 5)
- 6) JEAC 4601 Maximum Point-Oriented Degraded-Trilinear (PODT) bending model (model 6)
- 7) Hybrid Shear (HYS) model (model 7)
- 8) Hybrid Bending (HYB) model (model 8).

The CMS and CMB hysteretic models are based on a large wall test database including experiments done at the Los Alamos National Lab and at NCKU university in Taiwan (Cheng and Mertz, 1989). These CMS and CMB models were used in several of the research studies for nuclear industry as background for some of the DOE and ASCE standards.

The JEAC 4601 PO shear and PODT bending models are based on the Japan JEAC 4601-2015 App.3.7 guidance. The HYS and HYB models are developed in-house based on averaging at each time step of the computed hysteretic responses using the CMS and JEAC 4601 PO Shear models, and respectively, the CMB and the JEAC 4601 PODT bending models. Based on various comparisons against low-rise wall test data, the HYS and HYB models appears to provide the better fitting for the test data, as shown in Figure 16 (Oh et al, 2002).

The JEAC PO and PODT model damping is computed based on JEAC 4601-2015 App.3.7 that requires that the PO shear model has a zero-value hysteretic damping for the closed or stable hysteretic loops (see upper right plot in Figure 17). The PODT bending model permits only a limited hysteretic damping for the closed or stable hysteretic loops varying between zero hysteretic damping at the yielding point and 15% hysteretic damping at the ultimate point.

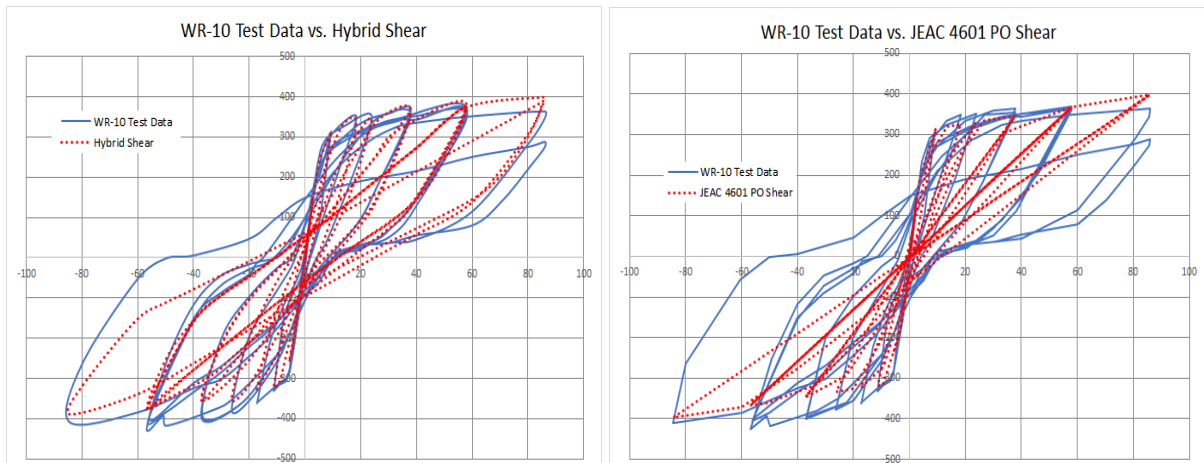


Figure 16 Hybrid Shear (HYS) Models Against Wall Test Data.

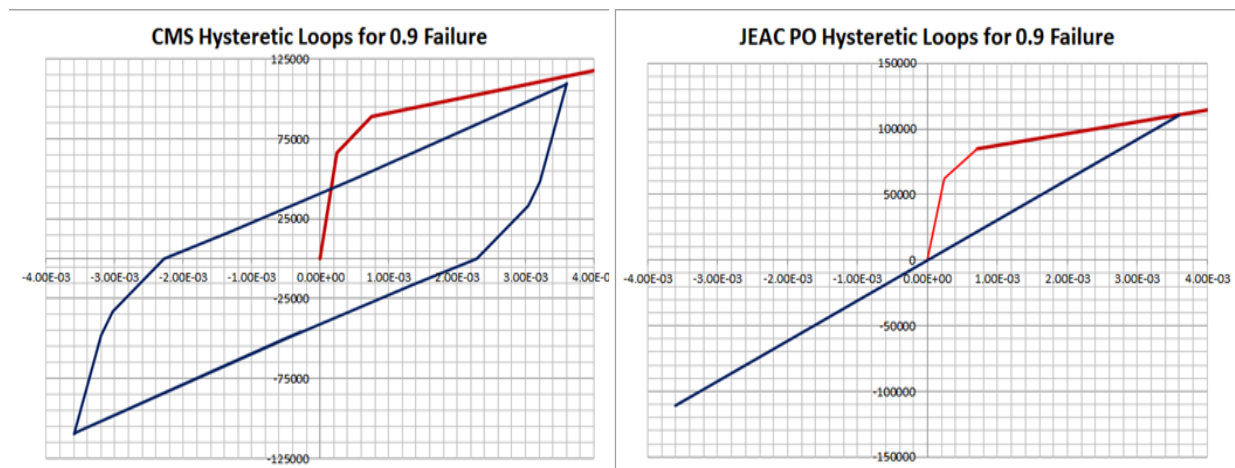


Figure 17 CMS and JEAC 4601 PO Shear Hysteretic Loops for A Harmonic Loading at 0.90 of Ultimate State Point (Conventional Failure Point)

Based on the hysteretic loops in Figure 16, the computed equivalent viscous damping for simulating the hysteretic energy loss is 19% for CMS, 9% for HYS, and zero-value for the JEAC 4601 PO Shear models. It should be noted that the using the closed loop area criterion, as shown in Figure 2, for

computing the equivalent-linear viscous damping is not applicable to PO Shear model since the closed loop area is zero. The ASCE 4-16 standard Section 3 recommends that for the Response Level 3 applicable to the BDBE levels, the total damping value up to 10% is acceptable. Otherwise, the analyst needs to justify larger damping values.

Alternatively, for the JEAC 4601 PO model, the equivalent viscous damping is computed based on the energy loss due plasticity or yielding during the earthquake (Chopra, 2006, Nitta et al., 2022). The JEAC 4601 damping requirements are based on a variety of wall tests performed in Japan for large, massive RC walls as those used for nuclear buildings (Taitokui, 1987).

It should be noted that using the NUPEC wall test data, the measured damping up to failure was not above 9% (Ichihara, 2022). It should be noted that often sophisticated nonlinear time-integration FEA codes could provide much higher damping values than the experimentally observed damping for the large size, massive RC walls used for nuclear buildings. Attention should be given to this key nonlinear modeling aspect since the damping values may significantly affect the computed structural seismic safety margins.

CONCLUDING REMARKS

This Part 1 paper introduces a practical nonlinear SSI analysis approach based on an iterative procedure that efficiently couples the equivalent-linear complex frequency SSI analysis with the nonlinear time-domain structure analysis. The iterative hybrid SSI approach is reasonably accurate and applicable to both the DBE and BDBE project applications.

The overall nonlinear SSI analysis implementation follows the Japanese seismic engineering practice for nonlinear modeling of the RC wall structures, being applicable to either detailed 3DFEM or lumped-parameter SR/Stick SSI models. Independent verification and validation studies, as mentioned herein, indicated that the iterative SSI approach provides a reasonable accuracy with high numerical efficiency.

The application of the iterative SSI approach using the ACS SASSI Option NON software is further described in the Part 2 companion paper.

REFERENCES

- American Concrete Institute (2020), *Building Code Requirements for Structural Concrete and Commentary*, ACI 318-19 Standard
- American Society of Civil Engineers (2017), *Seismic Analysis for Safety-Related Nuclear Structures and Commentary*, ASCE 4-16 Standard
- Architectural Institute of Japan (2018). *Technical Report for Modeling of Reinforced Concrete Structures*, AIJ RC Standard
- Chadwell, C.B. and Imbsen, R.A. (2004). *XTRACT: A Tool for Axial Force - Ultimate Curvature Interactions*, Structures 2004 on Building on Past, Securing Future, Nashville, TN, May 22-26
- Cheng, Y.F. and Mertz, G. (1989). *Inelastic Seismic Response of Reinforced Concrete Low-Rise Shear Walls of Building Structures*, University of Missouri-Rolla, Civil Engineering, CE 89-30
- Chopra, A. K. (2006). *Dynamics of Structures*, 3rd Edition, Prentice Hall International Series
- Gergely, P (1984). *Seismic Fragility of Reinforced Concrete Structures and Components for Application in Nuclear Facilities*, Published as NUREG/CR-4123
- Ghiocel, D. (2015). *Fast Nonlinear Seismic SSI Analysis Using a Hybrid Time-Complex Frequency Approach* Frequency Approach for Low-Rise Nuclear Concrete Shearwall Buildings, in Proc. SMiRT23 conference, Manchester, UK, August.
- Ghiocel, D. M. (2022). *Efficient Linear and Nonlinear Seismic SSI Analysis of Deeply Embedded Structures Using Flexible Reduced-Order Modeling (FVROM)*, SMiRT26 Conference, Div. 5, Berlin/Potsdam, Germany, July 10-15
- Ghiocel, D.M, Nitta, Y., Ikeda, R. and Shono, T (2022). *Seismic Nonlinear SSI Approach Based on Best Practices in US and Japan. Part 2: Application*, SMiRT26, Special Session on Nonlinear Seismic SSI Analysis Based on Best Practices in US and Japan, Berlin, July 10-15

- GP Technologies, Inc. (2022). *ACS SASSI NQA Version 4 User Manual, Including Advanced Options A-AA, NON, PRO, RVT-SIM and UPLIFT*, Revision 7, Rochester, NY, January 31.
- Gulec, C.K. and A.S. Whittaker (2009). *Performance-Based Assessment and Design of Squat Reinforced Concrete Shear Walls*, Technical Report MCEER, No. 09-0010
- Ichihara, Y., Nakamura, N, Nabeshima, K., Choi, B. and Nishida, A. (2022). *Applicability of Equivalent Linear Three-Dimensional FEM Analysis for Reactor Building to Seismic Response of Soil-Structure Interaction System*, SMiRT26 Conference, Special Session on Nonlinear Seismic SSI Analysis Based on Best Practices in US and Japan, Berlin, July 10-15
- Nitta, Y., Ikeda, R., Horiguchi, T. and Ghiocel, D.M. (2022). *Comparative Study Using Stick and 3DFEM Nonlinear SSI Models per JEAC 4601-2015 Recommendations*, SMiRT26, Special Session on Nonlinear Seismic SSI Analysis Based on Practices in US and Japan, July 10-15
- Nuclear Standard Committee of Japan Electric Association (2016), *Technical Code for Aseismic Design of Nuclear Power Plants*, Japan Electric Association Code (JEAC 4016-2015)
- Oh, Han and Lee (2002). *Effect of Boundary Element Details on the Seismic Deformation Capacity of Structural Walls*, J. of Earth. Engineering and Struct. Dynamics, 2002, Vol. 31:1583–1602.
- Reed J.W. and Kennedy R.P (1994). *Methodology for Developing Seismic Fragilities*, EPRI, Published in EPRI TR# 103959, Palo Alto, CA
- Spacone, Enrico, V Ciampi, FC Filippou (1992). *A Beam Element for Seismic Damage Analysis*, Report UCB/EERC-92/07, EERC, College of Engineering, University of California, Berkeley
- Taitokui, M. (1987). *Restoring Force Characteristics for RC Structure Walls* (in Japanese), Technical Report for Architectural Institute of Japan and Japan Atomic Energy Agency.